microbial biotechnology

Open Access

Attenuator LRR – a regulatory tool for modulating gene expression in Gram-positive bacteria

Xia Cai[1] Qian Wang,[1] Yu Fang,[1] Die Yao,[1] Yunda Zhan,[1] Baoju An,[1] Bing Yan[1] and Jun Cai[1,2,3]

[1]*Department of Microbiology, College of Life Sciences, Nankai University, Tianjin, 300071, China.*

[2]*Key Laboratory of Molecular Microbiology and Technology, Ministry of Education, Tianjin, 300071, China.*

[3]*Tianjin Key Laboratory of Microbial Functional Genomics, Tianjin, 300071, China.*

Summary

With the rapid development of synthetic biology in recent years, particular attention has been paid to RNA devices, especially riboswitches, because of their significant and diverse regulatory roles in prokaryotic and eukaryotic cells. Due to the limited performance and context-dependence of riboswitches, only a few of them (such as theophylline, tetracycline and ciprofloxacin riboswitches) have been utilized as regulatory tools in biotechnology. In the present study, we demonstrated that a ribosome-dependent ribo-regulator, LRR, discovered in our previous work, exhibits an attractive regulatory performance. Specifically, it offers a 60-fold change in expression in the presence of retapamulin and a low level of leaky expression of about 1–2% without antibiotics. Moreover, LRR can be combined with different promoters and performs well in *Bacillus thuringiensis*, *B. cereus*, *B. amyloliquefaciens*, and *B. subtilis*. Additionally, LRR also functions in the Gram-negative bacterium *Escherichia coli*. Furthermore, we demonstrate its ability to control melanin metabolism in *B. thuringiensis* BMB171. Our results show that LRR can be applied to regulate gene expression, construct genetic circuits and tune metabolic pathways, and has great potential for many applications in synthetic biology.

Received 9 November, 2020; revised 24 February, 2021; accepted 24 February, 2021.
For correspondence. E-mail: caijun@nankai.edu.cn; Tel./Fax: +86 22 23505964.
Microbial Biotechnology (2021) **14**(6), 2538–2551
doi:10.1111/1751-7915.13797
Funding information
This work was supported by the National Key Research and Development Program of China (No. 2018YFA0900100), and the National Natural Science Foundation of China (No. 31670081).

Introduction

Over recent decades, the field of synthetic biology has undergone considerable growth. It aims to predict, create and control cellular behaviour in a rationally engineered way (Cameron *et al.,* 2014; Green *et al.,* 2014). Regulatory devices providing fine-tuned and optimized regulatory behaviour have been investigated within synthetic biology to regulate gene expression and construct synthetic networks (Groher *et al.,* 2019). This has resulted in the development of protein-based inducible promoters (Lutz and Bujard, 1997), riboswitches (Serganov and Nudler, 2013; Boussebayle *et al.,* 2019; Chi *et al.,* 2019), and synthetic toehold switches (Green *et al.,* 2014), as well as many other types of component.

Protein-based inducible promoters allow the regulation of gene expression by up to a thousand-fold range, such as the IPTG-induced *lac* promoter, the arabinose-activated *ara* promoter, and the tetracycline-induced *tet* promoter (Lutz and Bujard, 1997). They have been widely employed to tune conditional protein expression in *E. coli*. However, inducible promoters are often subject to high rates of leaky expression, require transcription factors to function well (Hansen *et al.,* 1998; Giacalone *et al.,* 2006; Zhang *et al.,* 2012; Rosano and Ceccarelli, 2014) and can cause metabolic burden upon the host cell because of the cost of translation of the transcription factors (Kent and Dixon, 2019). Additionally, limitations have been observed when these regulatory elements are employed in diverse hosts (Fukui *et al.,* 2011). For example, protein-based regulatory tools derived from *E. coli* have been often found to not function well in other bacteria, such as *B. subtilis* (Cui *et al.,* 2016).

To avoid the limitations of protein-based regulatory tools, RNA-based regulatory tools have been increasingly viewed as excellent candidates to tune and control gene expression in synthetic biology (Ma *et al.,* 2014). Non-coding RNAs are essential tools to regulate cellular processes. They have distinct advantages over protein-based systems, such as fast regulatory response, genetic modularity, portability and the possibility of being combined with other platforms (Chappell *et al.,* 2017; Boussebayle *et al.,* 2019). Among these tools, riboswitches and RNA regulators that use base pairing (such as small transcription activating RNAs (STARs), toehold repressors, three-way junction (3WJ) repressors, and toehold switches) are believed to hold potential for

application in synthetic biology (Chappell *et al.,* 2017; Kim *et al.,* 2019; Chau *et al.,* 2020).

Riboswitches are newly discovered *cis*-modulatory elements controlling various basic metabolisms of living cells (McCown *et al.,* 2017). They consist of two connected RNA parts (Suess *et al.,* 2004), an aptamer domain that senses and binds a target ligand with high affinity and specificity, and an expression platform that undergoes a conformational change to control gene expression after ligand binding (Goodson *et al.,* 2017; Shanidze *et al.,* 2020). Riboswitches recognize a wide array of small metabolites, antibiotics and ions in cells, and directly tune gene expression based on the concentration of the specific ligand. They utilize various mechanisms to modulate target gene expression, such as sequestering or freeing the ribosome binding site (RBS), attenuating RNA transcription, splicing regulation and influencing RNA stability (Serganov and Nudler, 2013; Breaker, 2018; Pavlova *et al.,* 2019). These attractive advantages have resulted in riboswitches showing great promise as regulatory tools and are being widely explored and developed for applications in synthetic biology (Chi *et al.,* 2019). However, their limited dynamic range and context-sensitive performance often restrict their utility (Dwidar and Yokobayashi, 2019; Kent and Dixon, 2019). Additionally, the application of riboswitches in bacteria with different genetic contexts raises the problem of conformational stability (Chen *et al.,* 2012). Moreover, the cognate ligands of natural riboswitches are small metabolites and metal ions, which might be competitively bound by other factors. As a result, the expression of the target gene might not be tuned by its ligand in a predicted dose-dependent manner (Nshogozabahizi *et al.,* 2019). Thus, a small fraction of riboswitches is suitable for application and most synthetic riboswitches have only been used for proof-of-concept studies (Nshogozabahizi *et al.,* 2019). The bottleneck of synthetic riboswitch development may be the screening of fit-for-purpose aptamers possessing both excellent binding properties and conformational flexibility (Groher *et al.,* 2018).

In contrast, RNA regulators modulating gene expression through Watson-Crick base pairing can provide a more than 100-fold change in gene expression upon activation, for example, functioning as toehold switches (Callura *et al.,* 2010; Green *et al.,* 2014; Green *et al.,* 2017), toehold repressors, 3WJ repressors (Kim *et al.,* 2019), STARs (Chappell *et al.,* 2017; Bartoli *et al.,* 2020a), RNA transcription–translation regulators (Westbrook and Lucks, 2017), and tunable expression systems (Bartoli *et al.,* 2020b) plus many more.

All these RNA regulators comprise two separate RNA parts driven by different promoters. One RNA sequence in the 5′-untranslated region of the target gene controls gene transcription or translation by forming a terminator or sequestering the RBS, while the other plays a role in activating or repressing the expression of the target gene by changing the structure of the first RNA through base pairing. Toehold switches, toehold repressors and 3WJ repressors consist of a designed switch RNA and trigger RNA. The switch RNA lies upstream of the target gene. When the trigger RNA binds to the switch RNA, the latter will refold and change the accessible state of the RBS, thus regulating gene expression. These tools tune gene expression only at the translation level (Callura *et al.,* 2010; Green *et al.,* 2014; Kim *et al.,* 2019). Additionally, STARs, a powerful class of RNA-based transcriptional activators, comprise a target RNA located upstream of the gene of interest and a STAR (Chappell *et al.,* 2017). In the OFF state, the target RNA folds into an intrinsic terminator structure that inhibits transcription of the downstream gene, whereas in the ON state, a STAR is transcribed that interacts with the target RNA through base pairing, preventing terminator hairpin formation and allowing transcription of the downstream gene (Chappell *et al.,* 2017). Excitingly, RNA regulators based on base pairing can be designed computationally allowing for large libraries to be constructed and offer high-performance and orthogonal gene expression regulation in diverse contexts (Chappell *et al.,* 2017), which is difficult for riboswitches. However, one drawback of RNA regulators is that their two RNA parts are driven by different promoters, which enlarges and complicates the genetic circuits.

RNA-based attenuators have been known about for several decades. An attenuator is a *cis*-regulatory RNA element located in the 5'-untranslated region of its downstream gene, and controls gene expression by sensing antibiotics and amino acid starvation (Konan and Yanofsky, 1997; Dar *et al.,* 2016). In the presence of antibiotics and amino acid starvation conditions, the RNA structure of the attenuator changes upon transient ribosome stalling, which forms an anti-terminator or anti-sequester structure to generate a high expression level of the downstream gene. Most inducers of attenuators are antibiotics like lincomycin (Dar *et al.,* 2016; Duval *et al.,* 2018), tetracycline (Wang *et al.,* 2005), chloramphenicol (Bruckner and Matzura, 1985), erythromycin (Duval *et al.,* 2018) and so on. Additionally, some attenuators are induced upon amino acid starvation, such as a lack of tryptophan (Konan and Yanofsky, 1997). There has been little reported research on the application of attenuators.

In this study, we show that the attenuator, LRR, reported in our previous publication, offers a satisfactory fold change over 60-fold and a low rate of leakage expression of less than 2%. Moreover, LRR exhibited a fine regulatory performance when combined with

different promoters and successfully controlled melanin metabolism in its natural host *B. thuringiensis* BMB171. LRR can also play a switching role in *B. cereus*, *B. amyloliquefaciens*, *B. subtilis*, and *E. coli*. Therefore, we believe that attenuator LRR has potential as a candidate tool for synthetic biology.

Results

A natural ribosome-dependent attenuator with excellent regulatory behaviour

In our previous study, we identified a ribosome-dependent attenuator, termed LRR, which regulates the *rppA* gene (encoding a ribosomal protection protein) expression in *B. thuringiensis* BMB171 (Cai *et al.,* 2020). Attenuator LRR consists of a simple RNA part and modulates gene expression through conformational change resulted from transient ribosome stalling. In the presence of antibiotics chloramphenicol (Cam) or virginiamycin (Vgm), LRR is in the 'on' state and leads to increased expression of the downstream gene (Fig. 1A; Cai *et al.,* 2020). To gain a deeper understanding of the characteristics of LRR, other ribosome-targeting antibiotics were tested to induce the 'on' state of LRR. The results demonstrated that antibiotics retapamulin (Rtm), Vgm, Cam, pristinamycin IA (Pnm) and linezolid (Lnz) markedly induced the 'on' state of LRR (Fig. 1B). Among them, Rtm caused an increase in expression of over 60-fold. Regulatory performances of certain natural and synthetic riboswitches commonly used in synthetic biology were analysed and recorded in Table 1. The performance of LRR induced by Rtm is superior to most reported natural and synthetic riboswitches. Therefore, LRR is considered as a promising potential tool for application in synthetic biology. Next, we explored its regulatory performance when driven by Rtm.

Characterization of the dose dependence and activation ratio of LRR

To examine whether the switching activity of LRR is dependent on the dose of antibiotic Rtm, we used the previously engineered strain BMB171/pB-PLR, which carries the *rppA* promoter and LRR fused to the *lacZ* gene (Cai *et al.,* 2020). The strain was cultured in 20 ml of Luria-Bertani (LB) medium supplemented with different concentrations of Rtm for 6 h. Then, the β-galactosidase activities were measured to determine the dose dependency. The LacZ expression level was enhanced as the concentration of Rtm increased from 0 to 0.7 μg ml^{-1} and then decreased gradually when the Rtm concentration increased from 0.8 to 2 μg ml^{-1} (Fig. 2A). These results suggested that the appropriate dose of Rtm induced a higher expression level of LacZ.

To check for non-specific effects of Rtm, the β-galactosidase activities of strain BMB171/pB-P treated with different concentrations of Rtm (0, 0.5, and 0.7 μg ml^{-1}) were measured. Plasmid pB-P harbours the same promoter P*rppA* and RBS as pB-PLR, but has no LRR. The results demonstrated that Rtm did not significantly affect the activity of promoter P*rppA* (Data S1). Therefore, the higher expression of LacZ in strain BMB171/pB-PLR induced by Rtm resulted from the presence of attenuator LRR. Interestingly, a low concentration of Rtm promoted the growth of bacteria rather than inhibited it (Fig. 2C). This might be because of the stimulatory effect of a low dose of toxic substances, termed hormesis (Calabrese and Baldwin, 2003).

The fold change in expression caused by 0.5 μg ml^{-1} Rtm was about 63.9-fold, while that of 0.7 μg ml^{-1} Rtm was only about 66.5-fold. Therefore, for reasons of economy, Rtm at 0.5 μg ml^{-1} was selected to activate LRR. Then, the activation ratio elicited by Rtm was investigated. Strain BMB171/pB-PLR was incubated in 20 ml^{-1} of LB medium supplemented with 0.5 μg ml^{-1} Rtm for 16 h, and the LacZ expression and growth curve of the bacteria were quantified at the indicated time points. The result indicated that the *lacZ* expression level increased gradually during the induction period (Fig. 2B). After 16 h of induction, the activation ratio was about 64.4. Activation ratio is calculated by dividing the Miller units (β-galactosidase activity) in the presence of Rtm by the Miller units in the absence of Rtm. The strain BMB171/pB-PLR grew similarly in LB medium with or without 0.5 μg ml^{-1} Rtm (Fig. 2D).

Characterization of the leaky expression of LRR

In this study, leaky expression was evaluated by assessing the expression of a *lacZ* reporter gene driven by the 'off' state of LRR without antibiotics. Leaky expression was calculated by dividing the Miller units (β-galactosidase activity) in the presence of LRR by the Miller units in the absence of LRR. The result showed that the leaky expression level was about 0.8% when LRR was driven by its natural promoter P*rppA* derived from the *rppA* gene (Fig. 3A). Furthermore, the leaky expression of LRR driven by other promoters was also explored. The P*rppA* promoter was replaced with other promoters (P^{M}, P*yifA*, and P*yhfH*) in plasmids pB-P and pB-PLR to generate plasmids pB-P^{M}, pB-P^{M}LR, pB-P*yifA*, pB-P*yifA*-LR, pB-P*yhfH*, and pB-P*yhfH*-LR, respectively. P^{M} is the mutant of promoter P*rppA* with a higher activity than P*rppA*. P*yhfH* was derived from gene BMB171_RS05540 with lower activity than P*rppA*, while P*yifA* was derived from gene *yifA* encoding a sigma (54) modulation protein, and its activity is similar to P*rppA*. Results showed that the leaky expression of LRR driven

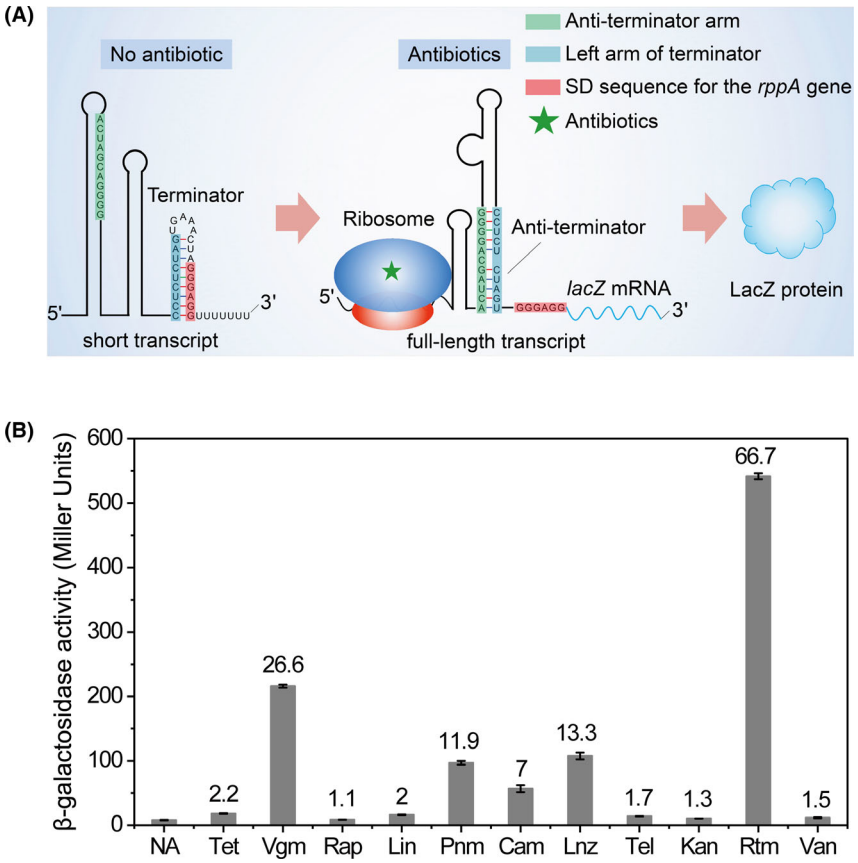

Fig. 1. Attenuator LRR is of good regulatory performance.
A. Regulation mechanism of the attenuator LRR. LRR forms a terminator structure under no antibiotic condition, which inhibits the transcription of *lacZ* mRNA and generates short transcripts. In the presence of antibiotics, ribosome stalling induced by antibiotics results in the formation of an anti-terminator structure of LRR. Consequently, the expression of *lacZ* is increased obviously.
B. Antibiotics induce LacZ expression. NA, no antibiotics; Tet, tetracycline (1 μg ml^{-1}, 2.25 μM); Vgm, virgimycin M (1 μg ml^{-1}, 1.903 μM); Rap, rapamycin (8 μg ml^{-1}, 8.751 μM); Lin, lincomycin (4 μg ml^{-1}, 9.839 μM); Pnm, pristinamycin IA (4 μg ml^{-1}, 4.614 μM); Cam, chloramphenicol (1 μg ml^{-1}, 3.095 μM); Lnz, linezolid (0.2 μg ml^{-1}, 0.593 μM); Tel, telithromycin (2.5 μg ml^{-1}, 3.079 μM); Kan, kanamycin (2 μg ml^{-1}, 3.433 μM); Rtm, retapamulin (0.5 μg ml^{-1}, 0.965 μM); Van, vancomycin (1.5 μg ml^{-1}, 1.01 μM). The numbers above the columns are the fold change induced by antibiotics. The fold change was calculated by dividing the Miller units under antibiotic conditions by the Miller units under no antibiotic condition.

by promoters P^{M}, P*yifA*, and P*yhfH* was 1.3, 1.8, and 1.4%, respectively (Fig. 3A). Therefore, LRR has little leakage, making it suitable for many synthetic biology applications.

Regulatory behaviour of LRR driven by different promoters

For an inducible expression system to be broadly useful, it is important that it functions well when used in combination with other genetic elements (Boussebayle *et al.,* 2019). Subsequently, regulatory behaviour of LRR driven by other promoters was investigated. The fold change in expression induced when LRR was driven by promoters P^{M}, P*yifA*, and P*yhfH* was 44.3, 26.8, and 34.8, respectively (Fig. 3B). The data indicated that LRR has satisfactory regulatory behaviour when driven by other promoters. This compatibility characteristic represents another advantage of LRR when used to modulate diverse gene expression.

Investigating regulatory behaviour of LRR in other bacteria

For the LRR attenuator to be broadly applicable across synthetic biology, it is also important that it is able to function in other types of bacteria. Thus, we investigated regulatory behaviour of LRR in *B. subtilis*, *B. cereus*, and *B. amyloliquefaciens*. The results indicated that LRR driven by the P*rppA* promoter has satisfactory regulatory behaviour in *B. subtilis*, *B. cereus*, and *B. amyloliquefaciens*, displaying a fold change in expression of 30, 93.6, and 34, respectively (Fig. 4A). We also investigated regulatory behaviour of LRR when driven by a

Table 1. Regulatory performance of certain reported riboswitches.

Riboswitches	Organism	Inducer concentration	State (+ligand)	Fold-change	Synthetic/natural	References
Caprolactam riboswitch	*E. coli*	50 mM	ON	3.36	Synthetic	Jang *et al.* (2019)
Ciprofloxacin riboswitch	Yeast, human	1 mM	OFF	7.5	Synthetic	Groher *et al.* (2018)
Neomycin riboswitches	*Saccharomyces cerevisiae*	100 μM	OFF	7.5	Synthetic	Weigand *et al.* (2008)
Paromomycin riboswitch	*S. cerevisiae*	250 μM	OFF	8.5	Synthetic	Boussebayle *et al.* (2019)
Theophylline riboswitch	*B. subtilis*	8 mM	ON	6.8	Synthetic	Cui *et al.* (2016)
Tetracycline riboswitch	*S. cerevisiae*	250 μM	OFF	40	Synthetic	Groher *et al.* (2019)
Tetracycline riboswitch	*S. cerevisiae*	250 μM	OFF	6	Synthetic	Suess *et al.* (2003)
Theophylline riboswitch	*E. coli*	500 μM	ON	8	Synthetic	Desai and Gallivan (2004)
Theophylline riboswitch 8.1	*E. coli*	1 mM	ON	36	Synthetic	Lynch *et al.* (2007)
Theophylline riboswitch 8.1*	*E. coli*	1 mM	ON	59	Synthetic	Lynch and Gallivan (2009)
Theophylline riboswitch 12.1	*E. coli*	1 mM	ON	96	Synthetic	Lynch and Gallivan (2009)
Theophylline riboswitch	*E. coli*	1 mM	OFF	27	Synthetic	Topp and Gallivan (2008)
Pyrimido [4,5-d] pyrimidine-2,4-diamine riboswitch	*E. coli*	1 mM	ON	80	Synthetic	Kent and Dixon (2019)
Histamine riboswitch	Artificial cells	5 mM	ON	30.7	Synthetic	Dwidar *et al.* (2019)
Mg^{2+} riboswitch	*Salmonella enterica*	25 μM	OFF	25	Natural	Cromie *et al.* (2006)
Glycine riboswitch	*Clostridium pasteurianum*	0.1 mM	OFF	10.2	Natural	Zhou *et al.* (2019)
Lysine riboswitch	*E. coli*	1 mM	OFF	~ 10	Natural	Zhou and Zeng (2015)
pubE riboswitch (2-aminopurine - responsive)	*Geobacillus*					
thermoglucosidasius	2 mM	ON	~ 29		Synthetic	Marcano-Velazquez *et al.* (2019)
N-acetylneuraminic acid riboswitch	*E. coli*	12.9 mM	OFF	5.8	Synthetic	Pang *et al.* (2020)
Fluoride-responsive riboswitch	*Pseudomonas putida*	15 mM	ON	3.8	Natural	Calero *et al.* (2020)

constitutive promoter, P43, derived from *B. subtilis*. The changes in expression induced by LRR were 15 and 6.6-fold in *B. amyloliquefaciens* and *B. subtilis*, respectively. Therefore, LRR could be used to tune gene expression and control metabolic pathways in *B. subtilis*, *B. cereus*, and *B. amyloliquefaciens*.

Additionally, we observed regulatory behaviour of LRR in the Gram-negative bacterium *E. coli*, using *rfp* as the reporter gene. The LRR coding region and *rfp* were inserted into plasmid pET-28(a) to generate the plasmid pET-LRR-RFP, and the T7 promoter was used to drive gene expression. The *E. coli* strain BL21 harbouring pET-LRR-RFP was cultured with and without antibiotics Rtm, Cam, Pnm, Tet, and Vgm at 37°C for 10 h, and then 2 ml of these cultures were collected and suspended in phosphate-buffered saline (PBS). The fluorescence intensity of these samples was detected and normalized to the cell density. The results demonstrated that LRR driven by the T7 promoter could regulate gene expression in *E. coli*. With the addition of Rtm, the expression of RFP increased, and the expression of RFP increased by approximately ninefold (Fig. 4B).

Tight regulation of melanin metabolism using LRR

In *B. thuringiensis* BMB171, melanin metabolism involves three enzymes encoded by an operon containing the *hppD*, *fahA*, and *hmgA* genes (Fig. 5A). The product of *hppD* is 4-hydroxyphenylpyruvate dioxygenase (HppD), which catalyses the synthesis of homogentisate from 4-hydroxyphenylpyruvate. Homogentisate molecules are changed to melanin via spontaneous oxidation and polymerization (Yang *et al.,* 2018). The *hmgA* gene encodes homogentisate-1,2-dioxygenase (HmgA) that degrades homogentisate to 4-maleylacetoacetate, which is isomerized by maleylacetoacetate isomerase (MaiA) to fumarylacetoacetate. The *fahA* gene encodes fumarylacetoacetate hydrolase, which hydrolyses fumarylacetoacetate to fumarate and acetoacetate (Fig. 5B; Tan *et al.,* 2019). HppD is the key enzyme for melanin synthesis, while HmgA and FahA play a role in decreasing melanin production by degrading homogentisate. To test its effectiveness and compatibility to regulate bacterial metabolism, LRR was used to control melanin metabolism by tuning *hppD* expression.

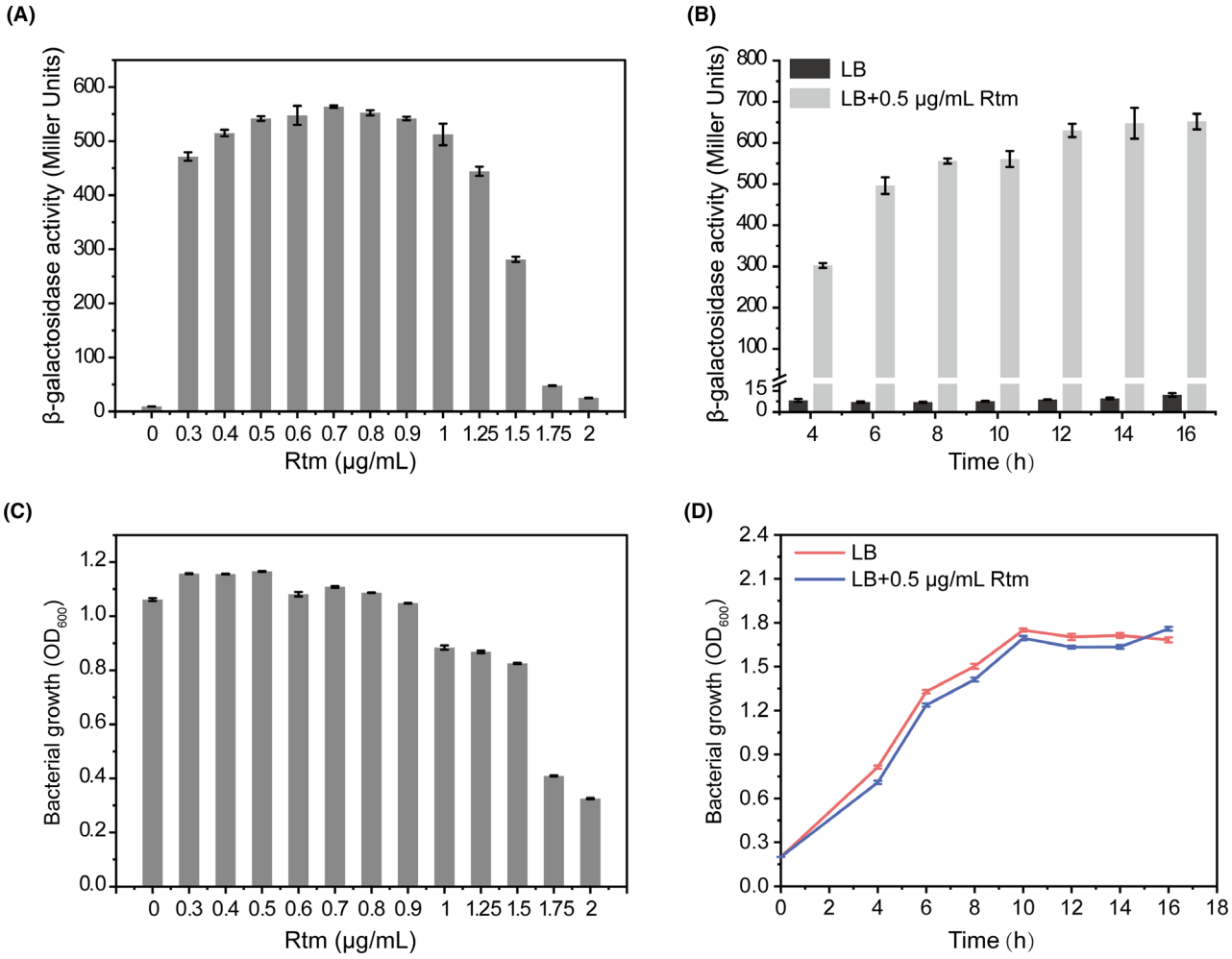

Fig. 2. Characterization of regulatory behaviour of LRR induced by Rtm in Bt BMB171.
A. The correlation between the dose of Rtm and LacZ expression.
B. The effect of Rtm (0.5 μg ml^{-1}, 0.965 μM) on LacZ expression at different time points.
C. The effect of treatment with different concentrations of Rtm for 6 h on Bt BMB171 growth.
D. Growth curve of BMB171/pB-PLR in LB medium added with or without Rtm (0.5 μg ml^{-1}, 0.965 μM). The *lacZ* expression level was measured by detecting β-galactosidase activity and calculated from three biologically independent replicates and shown as the mean ± SD. Cell density was evaluated using optical density at 600 nm (OD_{600}). The final concentrations of Rtm were shown as bellow: 0, 0.3 (0.579), 0.4 (0.772), 0.5 (0.965), 0.6 (1.1588), 0.7 (1.352), 0.8 (1.545), 0.9 (1.738), 1 (1.931), 1.25 (2.414), 1.5 (2.897), 1.75 (3.38) or 2 (3.863) μg ml^{-1} (μM)).

To assess the potential for LRR-based control of melanin metabolism, a high copy number plasmid pB-*hppD*, carrying LRR and *hppD*, was constructed and transformed into strain ΔHFA (Fig. 6A). Homogentisate molecules are not synthesized and degraded in strain ΔHFA because the genes *hppD*, *fahA* and *hmgA* have been deleted. Therefore, the production of melanin in strain ΔHFA/pB-*hppD* would be caused by the *hppD* gene in plasmid pB-*hppD*.

Strain ΔHFA/pB-*hppD* was cultured in LB medium (with 1% Tyr) supplemented with or without 0.5 μg ml^{-1} Rtm. Melanin production was assessed according to the optical density, and strain ΔHFA was used as the control. After treatment with 0.5 μg ml^{-1} Rtm for 24 h, the ΔHFA/pB-*hppD* culture turned dark brown, indicating that melanin had accumulated successfully in strain ΔHFA/pB-*hppD*. In contrast, the control group and the ΔHFA/pB-*hppD* strain without Rtm treatment cultured for the same time exhibited no melanin production. The optical densities at 400 nm (OD_{400}) of all strains at different time points are shown in Fig. 6B, and those of the cultures grown for 60 h are shown in Fig. 6D. Additionally, the inducible fold change in expression of the *hppD* gene at different time points was calculated using quantitative real-time reverse transcription PCR (qRT-PCR) data and shown in Fig. 6C. The expression of HppD

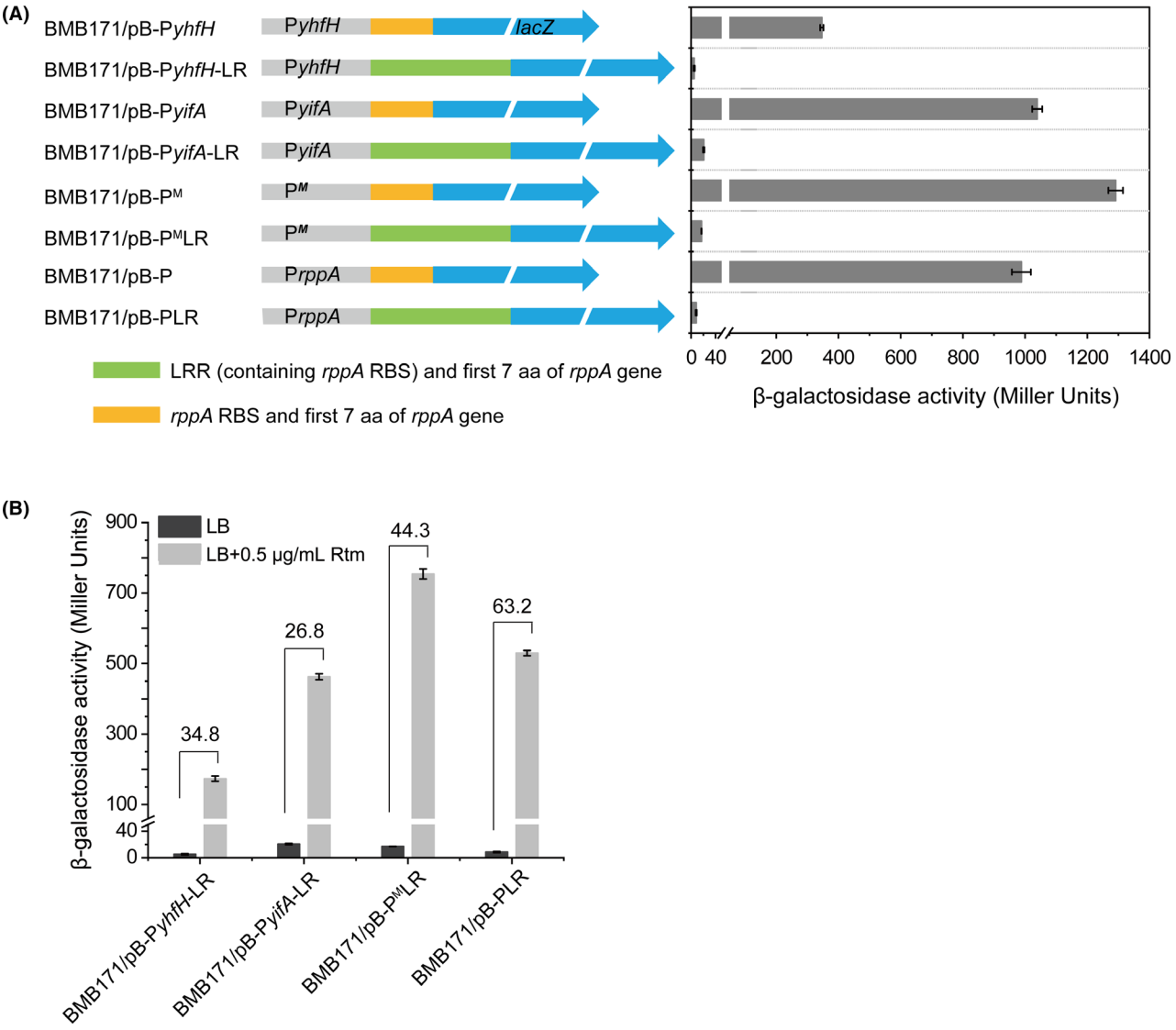

Fig. 3. Basal expression of LRR driven by different promoters.
A. The leaky expression level of LRR. Promoter and *lacZ* gene are indicated using a grey rectangle and light blue arrow, respectively. The fragment containing the LRR encoding region, *rppA* RBS, and the first 7 amino acids of the *rppA* gene is shown using a green rectangle. The fragment carrying RBS and the first 7 amino acids of the *rppA* gene is shown using an orange rectangle. aa, the abbreviation of amino acid. Take pB-PLR as an example, P, L, and R mean promoter, LRR and RBS of the *rppA* gene, respectively.
B. Regulatory behaviour of LRR driven by different promoters. The results are calculated from three biologically independent replicates and are shown as the mean ± SD. The numbers above the columns are the inducible fold and they were calculated by dividing the β-galactosidase activity in the presence of Rtm (0.5 μg ml^{-1}, 0.965 μM) by the corresponding β-galactosidase activity in the absence of Rtm.

protein was also detected using Western blotting with an anti-Flag antibody (Fig. 6E). These results demonstrated that LRR successfully controlled melanin metabolism by regulating the expression of the *hppD* gene.

Discussion

In the present study, we characterized a natural attenuator, LRR, as a promising genetic switch to control melanin metabolism. LRR displays > 60-fold change in expression (in the presence of Rtm) and a low rate of leaky expression (without Rtm). In addition, the compatible characteristics of LRR enable it to function well when driven by different promoters. Although LRR is derived from *B. thuringiensis*, it also exhibited good switching behaviour in *B. subtilis*, *B. cereus*, *B. amyloliquefaciens*, and *E. coli*. Therefore, LRR is a potentially useful regulatory tool for synthetic biology applications.

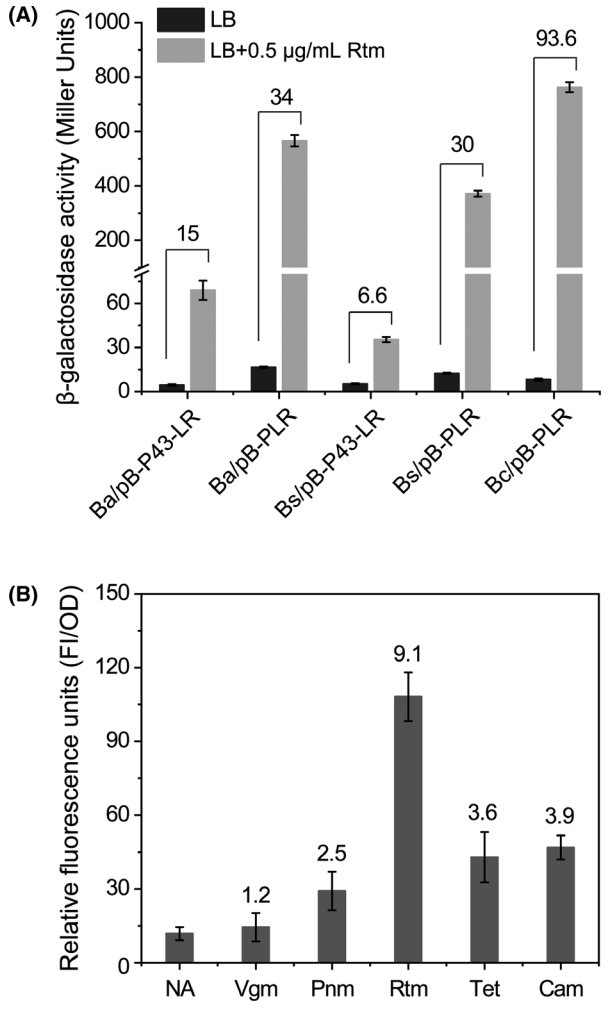

Fig. 4. Regulatory behaviour of LRR in different strains.
A. Regulatory behaviour of LRR in some Gram-positive bacteria. The numbers shown on the columns are the inducible fold, which were calculated by dividing the β-galactosidase activity in the presence of Rtm (0.5 μg ml^{-1}, 0.965 μM) by the corresponding β-galactosidase activity in the absence of Rtm. Ba, *B. amyloliquefaciens*; Bs, *B. subtilis*; Bc, *B. cereus*.
B. Regulatory behaviour of LRR in a Gram-negative bacterium *E. coli*. The expression level of RFP was represented by relative fluorescence units (FI/OD) calculated by dividing the fluorescence intensity (FI) by cell density (OD_{600}). The numbers shown on the columns are the activation ratios obtained by dividing the fluorescence intensity in the presence of antibiotics by the fluorescence intensity in the absence of antibiotics (NA, no antibiotics). Tet, 1 μg ml^{-1} (2.25 μM); Vgm, 2 μg ml^{-1} (3.806 μM); Pnm, 4 μg ml^{-1} (4.614 μM); Cam, 1 μg ml^{-1} (3.095 μM); Rtm, 2 μg ml^{-1} (3.86 μM). Results represent data from three biologically independent replicates and are shown as the mean ± SD.

Compared with most reported natural and synthetic riboswitches (Table 1), LRR possesses a higher capacity to induce a fold change in expression of the target gene. Attenuators and riboswitches are both *cis*-regulatory RNA elements that modulate gene expression by changing its spatial RNA structure. Similar to riboswitches, LRR-based regulation relies on a change in RNA conformation caused by transient ribosome stalling. This characteristic facilitates the manipulation and application of LRR in synthetic biology. However, compared with protein-basing regulators, synthetic theophylline riboswitches with a robust activation ratio (96-fold) (Table 1), and RNA regulators based on base pairing, the performance of the LRR attenuator has room for improvement. Fortunately, the background level of target gene expression driven by LRR is low; therefore, LRR is more suitable to control the expression of gene encoding proteins that have detrimental or repressive effects on bacteria. The directed evolution of a version of LRR with a higher activation ratio could be sought in the future to reduce the gap with other regulatory parts.

A riboswitch recognizes its ligand with high affinity and specificity, and its aptamer usually senses one metabolite or metal ion. Only a few riboswitches can recognize two ligands, such as the Ni^{2+}/Co^{2+} responsive riboswitch (Furukawa *et al.,* 2015). Compared with riboswitches, attenuator LRR is activated by several ribosome-targeting antibiotics, for example Vgm, Cam, Lnz, Pnm and Rtm. This behaviour may be an advantage, allowing multiple inputs to drive expression of a target gene in a dose-dependent manner. By comparison, small metabolites and metal ions sensed by riboswitches might not perform so predictably as they might bind competitively with other factors in bacteria.

Attenuators have been known about for several decades, and most of the previous studies focused on their working mechanism. In the presence of ribosome-targeting antibiotics or amino acid starvation, attenuators change their RNA structure through transient ribosome stalling and regulate downstream gene expression. This feature suggests that attenuators might only be suitable for bacteria because there is no spatial coupling between transcription and translation in eukaryotic cells (Gowrishankar and Harinarayanan, 2004; McGary and Nudler, 2013; Zhu *et al.,* 2019). According to our results, LRR could play a regulatory role in Gram-positive bacteria, such as *B. thuringiensis*, *B. subtilis*, *B. cereus*, *B. amyloliquefaciens*, as well as in Gram-negative bacterium *E. coli*. More bacteria should be tested in the future to determine if LRR maintains its regulatory role.

Attenuator LRR regulates the expression of an antibiotic resistance-associated protein RppA (Cai *et al.,* 2020); however, RppA does not seem to help bacteria improve their resistance to Rtm. However, unlike previously reported attenuators, LRR can promote significant increases in downstream gene expression. More importantly, the concentration of Rtm that can effectively induce LRR to refold has no significant detrimental effect on the host cells. Therefore, we believe that LRR has the potential to be applied as a regulatory tool. As the field of synthetic biology grows dramatically, the demand

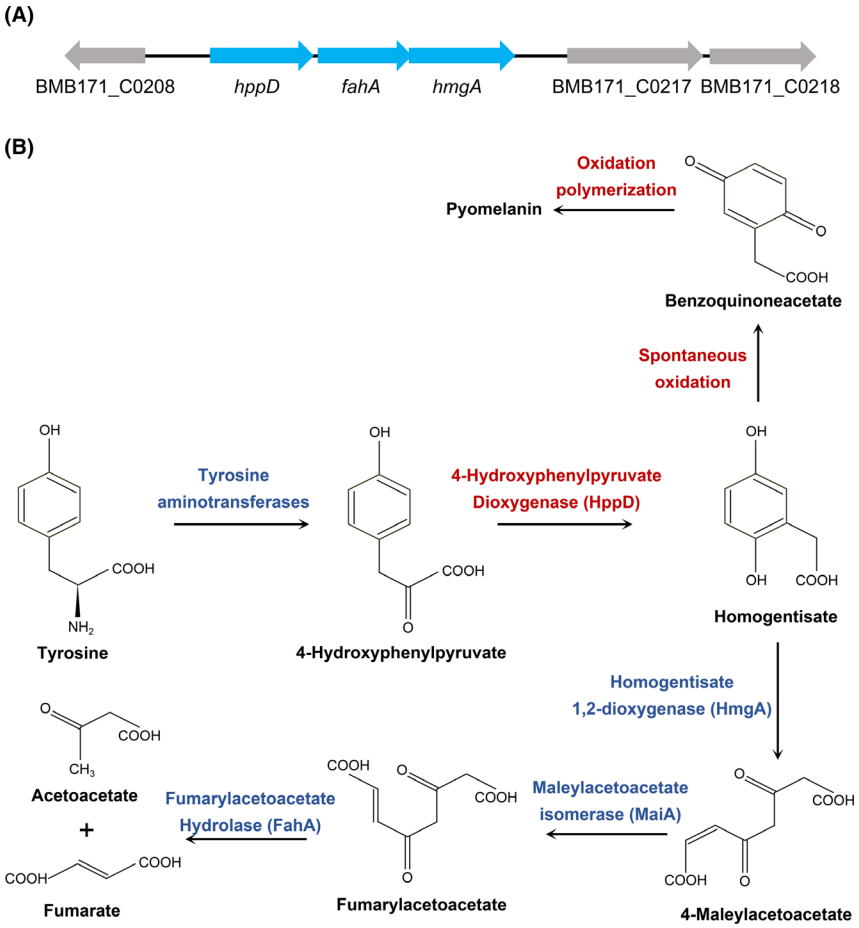

Fig. 5. Pathway for the synthesis of homogentisate (Yang *et al.*, 2018).
A. Genes *hppD*, *fahA*, and *hmgA* in BMB171 constitute an operon and are drawn using light blue arrow. Other genes are indicated using grey arrow.
B. Homogentisate pathway for the catabolism of tyrosine. Enzyme names for each step are indicated above the black arrows.

for regulatory tools is increasing. The discovery and application of attenuator LRR will enrich the variety of available switching tools and stimulate the discovery of other kinds of regulatory tools.

Experimental procedures

Primers, plasmids, bacterial strains and culture conditions

The primers, plasmids and bacterial strains used in this study are listed in Tables S1–S3 respectively. Primers were synthesized by GENEWIZ (Beijing, China). The *E. coli* strains were cultured in LB medium at 37°C with shaking at 200 r.p.m. *B. thuringiensis*, *B. cereus*, *B. subtilis* and *B. amyloliquefaciens* were incubated in LB medium at 28°C with shaking at 200 r.p.m. Ampicillin (GenStar, Beijing, China) (100 μg ml^{-1}) for *E. coli* and erythromycin (GenStar) (50 μg ml^{-1}) for *B. thuringiensis*, *B. cereus*, *B. subtilis* and *B. amyloliquefaciens* were supplemented as required.

Antibiotic-induction experiments

For the antibiotic-induction experiments, strains carrying certain plasmids were grown overnight in LB medium at 28°C with shaking at 200 r.p.m. Overnight cultures were diluted (OD_{600} = 0.2) in LB medium. Antibiotics Rtm, tetracycline (Tet), Vgm, rapamycin (Rap), lincomycin (Lin), Pnm, Cam, Lnz, telithromycin (Tel), kanamycin (Kan) and vancomycin (Van) (MedChem Express, Monmouth Junction, NJ, USA) were added as required and cultivation was continued for different times. Then, 2 ml of the cultures was harvested to assay the β-galactosidase activity or to extract the total RNA.

Plasmid construction

All constructs used in this study were based on the plasmids pHT1K or pET-28(a). The target DNA fragments were generated by PCR using the primers listed in Table S1. Then, DNA fragments containing the LRR

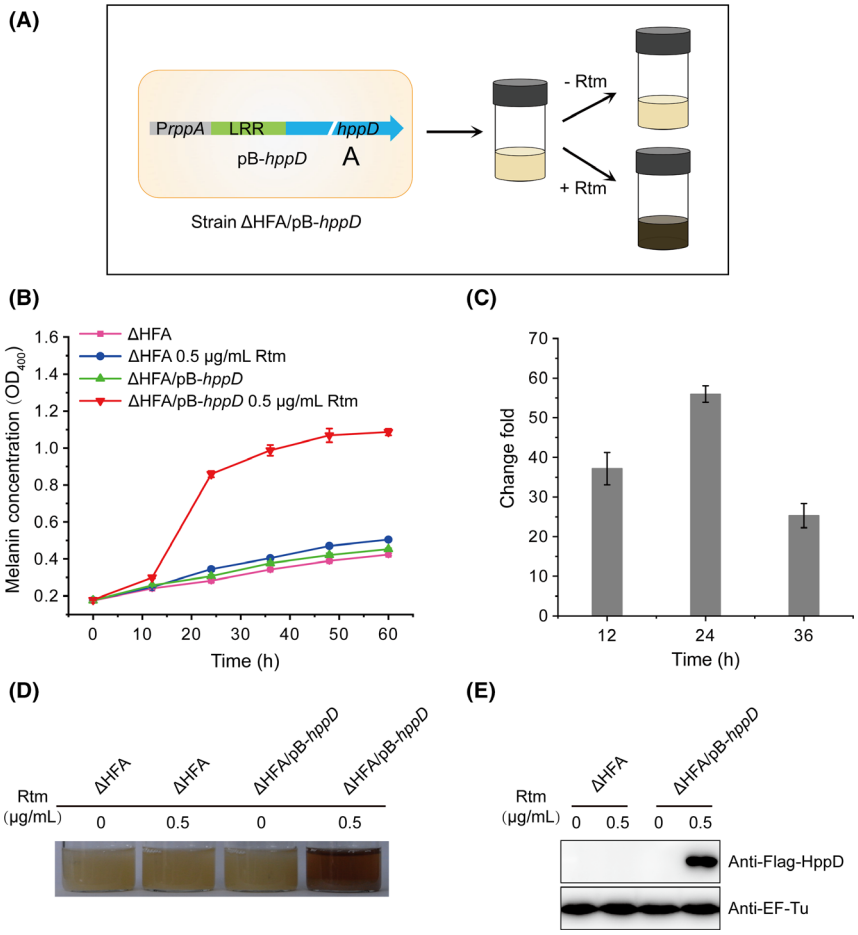

Fig. 6. Adopting LRR for tight regulation of melanin metabolism.
A. Schematic presentation of LRR application for controlling melanin synthesis. Gene *hppD* was fused to LRR and *rppA* promoter in high copy number plasmid pB-*hppD*. In the presence of Rtm, the strains harbouring plasmid pB-*hppD* produce melanin. Reversely, the melanin production is inhibited in the absence of Rtm.
B. The OD_{400} value of different strains in LB medium supplemented with or without 0.5 μg ml^{-1} Rtm. Strain ΔHFA was used as control.
C. Change folds of the *hppD* expression level induced by 0.5 μg ml^{-1} Rtm at different time points were measured using qRT-PCR. Change folds were obtained by dividing the relative expression level of the *hppD* gene in the presence of Rtm by the data in the absence of Rtm.
D. The culture supernatant of different strains with or without 0.5 μg ml^{-1} Rtm.
E. Western blotting of HppD fused with a Flag tag in different strains. Protein EF-Tu was used as a loading control.

coding region and promoters P^M, P*yhfH*, P*yifA* or P43 were ligated into plasmid pHT1K via the *Sal* I - *Nco* I sites to generate plasmids pB-P^MLR, pB-P*yhfH*-LR, pB-P*yifA*-LR and pB-P43-LR. Plasmid pB-PLR was constructed in a previous study (Cai *et al.,* 2020). Compared with plasmids pB-P^MLR, pB-P*yhfH*-LR, pB-P*yifA*-LR and pB-pLR, the LRR encoding region was deleted in plasmids pB-P^M, pB-P*yhfH*, pB-P*yifA* and pB-P, and their *lacZ* gene shares the *rppA* RBS. The sequences of the LRR coding region and all promoters used in this study are listed in the supplementary material.

Plasmid pB-*hppD* was generated by replacing the *lacZ* gene in plasmid pB-PLR with the *hppD* gene. A Flag-tag coding sequence was ligated to the 3′ end of the *hppD* gene, which encoded a Flag-tagged HppD protein that could be detecting using Western blotting. Plasmid pET-LRR-RFP was constructed by inserting the LRR coding region and the RFP open reading frame into plasmid pET-28(a) via the *Xba* I - *Xho* I sites. In plasmid pET-LRR-RFP, LRR and RFP expression were driven by a T7 promoter. All plasmids were constructed according to the manufacturer's instructions using the pEASY®-Basic Seamless Cloning and Assembly Kit (TransGen Biotech, Beijing, China), and all ligation reactions were transformed into *E. coli* DH5α competent cells. After confirmation by sequencing (GENEWIZ), recombinant plasmids were extracted from DH5α cells and transformed into the indicated competent cells via electroporation for further experiments.

β-galactosidase activity assay

The expression level of the LacZ protein in various strains was measured by determining β-galactosidase activity. The β-galactosidase activity was determined according to a previously described method and normalized to the cell density (Cai *et al.,* 2020). Two millilitres of bacterial cultures was subjected to centrifugation to collect the cells, which were suspended in 1 ml of Z-buffer (0.06 M Na_2HPO_4, 0.04 M NaH_2PO_4, 0.01 M KCl, 0.001 M $MgSO_4$, 0.05 M β-mercaptoethanol, pH 7.0). Then, cell disruption was performed using a Tissue Cell-destroyer 1000 (Hubei Xinzongke viral Disease Control Bio-Tech, Hubei, China). The treated sample (200 μl) was added with 800 μl of Z-buffer and then incubated at 37°C for 5 min. The reaction was activated by the addition of 200 μl of ortho-Nitrophenyl-β-galactoside (ONPG) at 37°C for 1–10 min, followed by adding 500 μl of 1 M Na_2CO_3 solution to stop the reaction. The reaction times were recorded. The absorbance of the reactions at 420 nm (OD_{420}) was measured using an EnSpire™ Multimode Plate Reader (Perkin-Elmer, Waltham, MA, USA). Finally, the OD_{420} value was converted into Miller units.

Fluorescence intensity assay

The expression of RFP for strains treated with or without antibiotics was measured by determining the fluorescence intensity. Cultures grown at 37°C with shaking at 200 r.p.m. for 10 h were centrifuged to assay fluorescence intensity. The collected bacterial cells from 2 ml cultures were washed with PBS three times and re-suspended in 1 ml of PBS. The fluorescence intensity of these suspensions was assayed in an EnSpire™ Multimode Plate Reader (Perkin-Elmer) using an excitation wavelength at 584 nm and an emission wavelength at 607 nm. The cell density (OD_{600}) of samples was also recorded. The expression level of RFP was represented by relative fluorescence units (FI/OD) calculated by dividing the fluorescence intensity (FI) by the cell density (OD).

Measurement of melanin production

To monitor melanin production, strains were incubated overnight in LB medium. The overnight cultures were diluted (OD_{600} = 0.2) in 20 ml of LB medium in a 250 ml flask and grown at 28°C with shaking at 200 r.p.m. Rtm was added to a final concentration of 0.5 μg ml^{-1}. Then, 2 ml of cultures grown for 12, 24, 36, 48 and 60 h was centrifuged and melanin production was determined by measuring the optical density at 400 nm (OD_{400}) using the EnSpire™ Multimode Plate Reader (Yang *et al.,* 2018).

Construction of the growth curve

The growth curve of strains was evaluated using their optical density at 600 nm (OD_{600}). The bacteria were cultured overnight in LB medium. The overnight cultures were diluted (OD_{600} = 0.2) in 20 ml of LB medium (in a 50 ml flask) supplemented with or without certain antibiotics, and incubated at 28°C with shaking at 200 r.p.m. Then, the optical density of the cultures was measured at different time points to construct the growth curve.

RNA extraction and qRT-PCR

Total RNA was extracted using the TRIzol reagent (Invitrogen, Waltham, MA, USA) and then quantified using NanoDrop technology (Thermo Scientific, Waltham, MA, USA). cDNA was synthesized using a PrimeScript™ RT reagent Kit with gDNA Eraser (Takara, Shiga, Japan) according to the manufacturer's instructions. The cDNA was then used as the template for quantitative real-time PCR (qPCR). The 16S rRNA gene was used as an internal control (Cai *et al.,* 2020).

Western blotting

Isolation of total bacterial proteins and determination of protein levels by Western blotting following SDS-PAGE were performed according to a previously described method (Jiang *et al.,* 2018). The primary rabbit monoclonal antibody recognized the Flag-tag (DYKDDDDK Tag (D6W5B)) (Cell Signaling Technology, Danvers, MA, USA) and the secondary antibody, horseradish peroxidase (HRP)-conjugated Goat Anti-Rabbit IgG (H + L) (ABclonal, Wuhan, China), were used to probe the Flag-HppD protein. EF-Tu served as a loading control (Duval *et al.,* 2018) and was probed using an anti-eEF1A1/EF-Tu primary antibody (Abcam, Cambridge, MA, USA) and an HRP-Goat Anti-Mouse IgG (H + L) secondary antibody (ABclonal).

Acknowledgements

J.C. and X.C. designed the study. X.C. carried out most of the experimental work and analysed the data. Q.W. and D.Y. constructed several plasmids. Y.F., B.A. and Y.Z. constructed the strain ΔHFA. X.C. wrote the manuscript. J.C., B.Y. and X.C. revised the manuscript. This work was supported by the National Key Research and Development Program of China (No. 2018YFA0900100), and the National Natural Science Foundation of China (No. 31670081).

Conflict of interest

None declared.

References

Bartoli, V., di Bernardo, M., and Gorochowski, T.E. (2020a) Self-adaptive biosystems through tunable genetic parts and circuits. *Curr Opin Syst Biol* **24:** 78–85.

Bartoli, V., Meaker, G.A., di Bernardo, M., and Gorochowski, T.E. (2020b) Tunable genetic devices through simultaneous control of transcription and translation. *Nat Commun* **11:** 2095.

Boussebayle, A., Torka, D., Ollivaud, S., Braun, J., Bofill-Bosch, C., Dombrowski, M., *et al*. (2019) Next-level riboswitch development-implementation of Capture-SELEX facilitates identification of a new synthetic riboswitch. *Nucleic Acids Res* **47:** 4883–4895.

Breaker, R.R. (2018) Riboswitches and translation control. *Cold Spring Harb Perspect Biol* **10:** a032797.

Bruckner, R., and Matzura, H. (1985) Regulation of the inducible chloramphenicol acetyltransferase gene of the *Staphylococcus aureus* plasmid pUB112. *EMBO J* **4:** 2295–2300.

Cai, X., Zhan, Y., Cao, Z., Yan, B., and Cai, J. (2020) Expression of ribosomal protection protein RppA is regulated by a ribosome-dependent ribo-regulator and two mistranslation products. *Environ Microbiol* **23:** 696–712.

Calabrese, E.J., and Baldwin, L.A. (2003) The hormetic dose-response model is more common than the threshold model in toxicology. *Toxicol Sci* **71:** 246–250.

Calero, P., Volke, D.C., Lowe, P.T., Gotfredsen, C.H., O'Hagan, D., and Nikel, P.I. (2020) A fluoride-responsive genetic circuit enables in *vivo* biofluorination in engineered *Pseudomonas putida*. *Nat Commun* **11:** 5045.

Callura, J.M., Dwyer, D.J., Isaacs, F.J., Cantor, C.R., and Collins, J.J. (2010) Tracking, tuning, and terminating microbial physiology using synthetic riboregulators. *Proc Natl Acad Sci USA* **107:** 15898–15903.

Cameron, D.E., Bashor, C.J., and Collins, J.J. (2014) A brief history of synthetic biology. *Nat Rev Microbiol* **12:** 381–390.

Chappell, J., Westbrook, A., Verosloff, M., and Lucks, J.B. (2017) Computational design of small transcription activating RNAs for versatile and dynamic gene regulation. *Nat Commun* **8:** 1051.

Chau, T.H.T., Mai, D.H.A., Pham, D.N., Le, H.T.Q., and Lee, E.Y. (2020) Developments of riboswitches and toehold switches for molecular detection-biosensing and molecular diagnostics. *Int J Mol Sci* **21:** 3192.

Chen, B., Zuo, X., Wang, Y.X., and Dayie, T.K. (2012) Multiple conformations of SAM-II riboswitch detected with SAXS and NMR spectroscopy. *Nucleic Acids Res* **40:** 3117–3130.

Chi, X., Zhang, S., Sun, H., Duan, Y., Qiao, C., Luan, G., and Lu, X. (2019) Adopting a theophylline-responsive riboswitch for flexible regulation and understanding of glycogen metabolism in *Synechococcus elongatus* PCC7942. *Front Microbiol* **10:** 551.

Cromie, M.J., Shi, Y., Latifi, T., and Groisman, E.A. (2006) An RNA sensor for intracellular Mg^{2+}. *Cell* **125:** 71–84.

Cui, W., Han, L., Cheng, J., Liu, Z., Zhou, L., Guo, J., and Zhou, Z. (2016) Engineering an inducible gene expression system for *Bacillus subtilis* from a strong constitutive promoter and a theophylline-activated synthetic riboswitch. *Microb Cell Fact* **15:** 199.

Dar, D., Shamir, M., Mellin, J.R., Koutero, M., Stern-Ginossar, N., Cossart, P., and Sorek, R. (2016) Term-seq reveals abundant ribo-regulation of antibiotics resistance in bacteria. *Science* **352:** aad9822.

Desai, S.K., and Gallivan, J.P. (2004) Genetic screens and selections for small molecules based on a synthetic riboswitch that activates protein translation. *J Am Chem Soc* **126:** 13247–13254.

Duval, M., Dar, D., Carvalho, F., Rocha, E.P.C., Sorek, R., and Cossart, P. (2018) HflXr, a homolog of a ribosome-splitting factor, mediates antibiotic resistance. *Proc Natl Acad Sci USA* **115:** 13359–13364.

Dwidar, M., Seike, Y., Kobori, S., Whitaker, C., Matsuura, T., and Yokobayashi, Y. (2019) Programmable artificial cells using histamine-responsive synthetic riboswitch. *J Am Chem Soc* **141:** 11103–11114.

Dwidar, M., and Yokobayashi, Y. (2019) Riboswitch signal amplification by controlling plasmid copy number. *ACS Synth Biol* **8:** 245–250.

Fukui, T., Ohsawa, K., Mifune, J., Orita, I., and Nakamura, S. (2011) Evaluation of promoters for gene expression in polyhydroxyalkanoate-producing *Cupriavidus necator* H16. *Appl Microbiol Biotechnol* **89:** 1527–1536.

Furukawa, K., Ramesh, A., Zhou, Z., Weinberg, Z., Vallery, T., Winkler, W.C., and Breaker, R.R. (2015) Bacterial riboswitches cooperatively bind Ni^{2+} or Co^{2+} ions and control expression of heavy metal transporters. *Mol Cell* **57:** 1088–1098.

Giacalone, M.J., Gentile, A.M., Lovitt, B.T., Berkley, N.L., Gunderson, C.W., and Surber, M.W. (2006) Toxic protein expression in *Escherichia coli* using a rhamnose-based tightly regulated and tunable promoter system. *Biotechniques* **40:** 355–364.

Goodson, M.S., Bennett, A.C., Jennewine, B.R., Briskin, E., Harbaugh, S.V., and Kelley-Loughnane, N. (2017) Amplifying riboswitch signal output using cellular wiring. *ACS Synth Biol* **6:** 1440–1444.

Gowrishankar, J., and Harinarayanan, R. (2004) Why is transcription coupled to translation in bacteria? *Mol Microbiol* **54:** 598–603.

Green, A.A., Kim, J., Ma, D., Silver, P.A., Collins, J.J., and Yin, P. (2017) Complex cellular logic computation using ribocomputing devices. *Nature* **548:** 117–121.

Green, A.A., Silver, P.A., Collins, J.J., and Yin, P. (2014) Toehold switches: de-novo-designed regulators of gene expression. *Cell* **159:** 925–939.

Groher, A.C., Jager, S., Schneider, C., Groher, F., Hamacher, K., and Suess, B. (2019) Tuning the performance of synthetic riboswitches using machine learning. *ACS Synth Biol* **8:** 34–44.

Groher, F., Bofill-Bosch, C., Schneider, C., Braun, J., Jager, S., Geissler, K., *et al*. (2018) Riboswitching with ciprofloxacin-development and characterization of a novel RNA regulator. *Nucleic Acids Res* **46:** 2121–2132.

Hansen, L.H., Knudsen, S., and Sorensen, S.J. (1998) The effect of the *lacY* gene on the induction of IPTG inducible promoters, studied in *Escherichia coli* and *Pseudomonas fluorescens*. *Curr Microbiol* **36:** 341–347.

Jang, S., Jang, S., Im, D.K., Kang, T.J., Oh, M.K., and Jung, G.Y. (2019) Artificial caprolactam-specific riboswitch as an intracellular metabolite sensor. *ACS Synth Biol* **8:** 1276–1283.

Jiang, K., Hou, X.Y., Tan, T.T., Cao, Z.L., Mei, S.Q., Yan, B., *et al*. (2018) Scavenger receptor-C acts as a receptor for *Bacillus thuringiensis* vegetative insecticidal protein Vip3Aa and mediates the internalization of Vip3Aa via endocytosis. *PLoS Pathog* **14:** e1007347.

Kent, R., and Dixon, N. (2019) Systematic evaluation of genetic and environmental factors affecting performance of translational riboswitches. *ACS Synth Biol* **8:** 884–901.

Kim, J., Zhou, Y., Carlson, P.D., Teichmann, M., Chaudhary, S., Simmel, F.C., *et al*. (2019) De novo-designed translation-repressing riboregulators for multi-input cellular logic. *Nat Chem Biol* **15:** 1173–1182.

Konan, K.V., and Yanofsky, C. (1997) Regulation of the *Escherichia coli tna* operon: nascent leader peptide control at the *tnaC* stop codon. *J Bacteriol* **179:** 1774–1779.

Lutz, R., and Bujard, H. (1997) Independent and tight regulation of transcriptional units in *Escherichia coli* via the LacR/O, the TetR/O and AraC/I1-I2 regulatory elements. *Nucleic Acids Res* **25:** 1203–1210.

Lynch, S.A., Desai, S.K., Sajja, H.K., and Gallivan, J.P. (2007) A high-throughput screen for synthetic riboswitches reveals mechanistic insights into their function. *Chem Biol* **14:** 173–184.

Lynch, S.A., and Gallivan, J.P. (2009) A flow cytometry-based screen for synthetic riboswitches. *Nucleic Acids Res* **37:** 184–192.

Ma, A.T., Schmidt, C.M., and Golden, J.W. (2014) Regulation of gene expression in diverse cyanobacterial species by using theophylline-responsive riboswitches. *Appl Environ Microbiol* **80:** 6704–6713.

Marcano-Velazquez, J.G., Lo, J., Nag, A., Maness, P.C., and Chou, K.J. (2019) Developing riboswitch-mediated gene regulatory controls in thermophilic bacteria. *ACS Synth Biol* **8:** 633–640.

McCown, P.J., Corbino, K.A., Stav, S., Sherlock, M.E., and Breaker, R.R. (2017) Riboswitch diversity and distribution. *RNA* **23:** 995–1011.

McGary, K., and Nudler, E. (2013) RNA polymerase and the ribosome: the close relationship. *Curr Opin Microbiol* **16:** 112–117.

Nshogozabahizi, J.C., Aubrey, K.L., Ross, J.A., and Thakor, N. (2019) Applications and limitations of regulatory RNA elements in synthetic biology and biotechnology. *J Appl Microbiol* **127:** 968–984.

Pang, Q., Han, H., Liu, X., Wang, Z., Liang, Q., Hou, J., *et al*. (2020) In *vivo* evolutionary engineering of riboswitch with high-threshold for N-acetylneuraminic acid production. *Metab Eng* **59:** 36–43.

Pavlova, N., Kaloudas, D., and Penchovsky, R. (2019) Riboswitch distribution, structure, and function in bacteria. *Gene* **708:** 38–48.

Rosano, G.L., and Ceccarelli, E.A. (2014) Recombinant protein expression in *Escherichia coli*: advances and challenges. *Front Microbiol* **5:** 172.

Serganov, A., and Nudler, E. (2013) A decade of riboswitches. *Cell* **152:** 17–24.

Shanidze, N., Lenkeit, F., Hartig, J.S., and Funck, D. (2020) A theophylline-responsive riboswitch regulates expression of nuclear-encoded genes. *Plant Physiol* **182:** 123–135.

Suess, B., Fink, B., Berens, C., Stentz, R., and Hillen, W. (2004) A theophylline responsive riboswitch based on helix slipping controls gene expression in *vivo*. *Nucleic Acids Res* **32:** 1610–1614.

Suess, B., Hanson, S., Berens, C., Fink, B., Schroeder, R., and Hillen, W. (2003) Conditional gene expression by controlling translation with tetracycline-binding aptamers. *Nucleic Acids Res* **31:** 1853–1858.

Tan, T.T., Zhang, X.D., Miao, Z., Yu, Y., Du, S.L., Hou, X.Y., and Cai, J. (2019) A single point mutation in *hmgA* leads to melanin accumulation in *Bacillus thuringiensis* BMB181. *Enzyme Microb Technol* **120:** 91–97.

Topp, S., and Gallivan, J.P. (2008) Riboswitches in unexpected places–a synthetic riboswitch in a protein coding region. *RNA* **14:** 2498–2503.

Wang, Y., Rotman, E.R., Shoemaker, N.B., and Salyers, A.A. (2005) Translational control of tetracycline resistance and conjugation in the *Bacteroides* conjugative transposon CTnDOT. *J Bacteriol* **187:** 2673–2680.

Weigand, J.E., Sanchez, M., Gunnesch, E.B., Zeiher, S., Schroeder, R., and Suess, B. (2008) Screening for engineered neomycin riboswitches that control translation initiation. *RNA* **14:** 89–97.

Westbrook, A.M., and Lucks, J.B. (2017) Achieving large dynamic range control of gene expression with a compact RNA transcription-translation regulator. *Nucleic Acids Res* **45:** 5614–5624.

Yang, W., Ruan, L., Tao, J., Peng, D., Zheng, J., and Sun, M. (2018) Single amino acid substitution in homogentisate dioxygenase affects melanin production in *Bacillus thuringiensis*. *Front Microbiol* **9:** 2242.

Zhang, F., Carothers, J.M., and Keasling, J.D. (2012) Design of a dynamic sensor-regulator system for production of chemicals and fuels derived from fatty acids. *Nat Biotechnol* **30:** 354–359.

Zhou, L., Ren, J., Li, Z., Nie, J., Wang, C., and Zeng, A.P. (2019) Characterization and engineering of a *Clostridium* glycine riboswitch and its use to control a novel metabolic pathway for 5-aminolevulinic acid production in *Escherichia coli*. *ACS Synth Biol* **8:** 2327–2335.

Zhou, L.B., and Zeng, A.P. (2015) Exploring lysine riboswitch for metabolic flux control and improvement of L-lysine synthesis in *Corynebacterium glutamicum*. *ACS Synth Biol* **4:** 729–734.

Zhu, M., Mori, M., Hwa, T., and Dai, X. (2019) Disruption of transcription-translation coordination in *Escherichia coli* leads to premature transcriptional termination. *Nat Microbiol* **4:** 2347–2356.

Supporting information

Additional supporting information may be found online in the Supporting Information section at the end of the article.

Table S1. Primers used in this study.

Table S2. Plasmids used in this study.

Table S3. Strains used in this study.

Data S1. The effect of Rtm on the activity of promoter PrppA. The activities of promoter PrppA treated with different concentrations of antibiotic Rtm were obtained by detecting β-galactosidase activity and calculated from three biologically independent replicates, and shown as the mean ± SD. ns, no significant difference, $P > 0.05$. Rtm, 0.5 μg/mL (0.965 μM), 0.7 μg/mL (1.352 μM).

